

Multipoint Measurement of Fine-Structured EMIC Waves by Arase, Van Allen Probe A, and Ground Stations

著者	Matsuda S., Miyoshi Y., Kasahara Y., Blum L., Colpitts C., Asamura K., Kasaba Y., Matsuoka A., Tsuchiya F., Kumamoto A., Teramoto M., Nakamura S., Kitahara M., Shinohara I., Reeves G., Spence H., Shiokawa K., Nagatsuma T., Oyama S., Mann I.R.
journal or publication title	Geophysical Research Letters
volume	48
number	23
page range	e2021GL096488-1-e2021GL096488-11
year	2021-11-10
URL	http://hdl.handle.net/10228/00009051

doi: <https://doi.org/10.1029/2021GL096488>

Geophysical Research Letters[®]

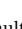





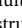






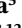


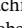



RESEARCH LETTER

10.1029/2021GL096488

Multipoint Measurement of Fine-Structured EMIC Waves by Arase, Van Allen Probe A, and Ground Stations

Key Points:

- The simultaneous multipoint observation of fine-structured electromagnetic ion cyclotron (EMIC) waves was achieved by Arase, Van Allen Probe, and two ground-based stations
- The growth of the observed fine-structured EMIC waves was associated with ambient electron density irregularities in the midlatitudes
- We investigated the spatial scale of the observed EMIC waves and their contribution to ion heating by utilizing the multipoint measurement

S. Matsuda¹ , Y. Miyoshi² , Y. Kasahara¹ , L. Blum³ , C. Colpitts⁴ , K. Asamura⁵ , Y. Kasaba⁶ , A. Matsuoka⁷ , F. Tsuchiya⁶ , A. Kumamoto⁶ , M. Teramoto⁸ , S. Nakamura² , M. Kitahara² , I. Shinohara⁵ , G. Reeves⁹ , H. Spence¹⁰ , K. Shiokawa² , T. Nagatsuma¹¹ , S. Oyama^{2,12} , and I. R. Mann¹³ 

¹Graduate School of Natural Science and Technology, Kanazawa University, Kanazawa, Japan, ²Institute for Space-Earth Environmental Research, Nagoya University, Nagoya, Japan, ³Laboratory for Atmospheric and Space Physics, University of Colorado Boulder, Boulder, CO, USA, ⁴School of Physics and Astronomy, University of Minnesota, Minneapolis, MN, USA, ⁵Institute of Space and Astronautical Science, Japan Aerospace Exploration Agency, Sagami, Japan, ⁶Graduate School of Science, Tohoku University, Sendai, Japan, ⁷Graduate School of Science, Kyoto University, Kyoto, Japan, ⁸Graduate School of Engineering, Kyushu Institute of Technology, Kitakyushu, Japan, ⁹Space Science and Applications Group, Los Alamos National Laboratory, Los Alamos, NM, USA, ¹⁰Institute for the Study of Earth, Oceans, and Space, University of New Hampshire, Durham, NH, USA, ¹¹National Institute of Information and Communications Technology, Koganei, Japan, ¹²National Institute of Polar Research, Tachikawa, Japan, ¹³Department of Physics, University of Alberta, Edmonton, AB, Canada

Supporting Information:

Supporting Information may be found in the online version of this article.

Correspondence to:

S. Matsuda,
matsuda@staff.kanazawa-u.ac.jp

Citation:

Matsuda, S., Miyoshi, Y., Kasahara, Y., Blum, L., Colpitts, C., Asamura, K., et al. (2021). Multipoint measurement of fine-structured EMIC waves by Arase, Van Allen Probe A, and ground stations. *Geophysical Research Letters*, 48, e2021GL096488. <https://doi.org/10.1029/2021GL096488>

Received 26 OCT 2021

Accepted 3 NOV 2021

Author Contributions:

Conceptualization: S. Matsuda

Data curation: S. Matsuda

Formal analysis: S. Matsuda

Investigation: S. Matsuda

Methodology: S. Matsuda

Project Administration: Y. Miyoshi, I. Shinohara

Abstract We examined the growth and propagation of fine-structured electromagnetic ion cyclotron (EMIC) waves related to time-varying density irregularities using multipoint measurement data observed by Arase, Van Allen Probe A, and two ground-based induction magnetometers (Gakona and Dawson) during a field line conjunction event on April 18, 2019. We analyzed the wave data obtained by the aforementioned spacecraft and stations, and found that the appearance of fine structures in the observed EMIC waves clearly coincided with the ambient electron density irregularities in the magnetosphere, which can cause periodic wave growth and waveguiding on their propagation. Furthermore, we found that the latitudinal widths of the EMIC wave activity region and the wave propagation duct were ~185 km and less than 80 km at an auroral altitude of 100 km, respectively. We also found thermal ion heating (< 200 eV/q) during the EMIC wave activity.

Plain Language Summary Electromagnetic ion cyclotron (EMIC) waves are an important plasma waves that control energetic ion and relativistic electron precipitations in the terrestrial inner magnetosphere. We investigated the growth and propagation of fine-structured EMIC waves observed simultaneously by two spacecraft (Japanese Arase and U.S. Van Allen Probe A) and two ground stations (Gakona and Dawson). The two spacecraft orbited along the same field line, and we measured the same fine-structured EMIC waves in different geomagnetic latitude regions. The same EMIC waves were observed at the two ground stations located near the magnetic footprints of the two spacecraft. We report that the periodic growth of the observed EMIC waves was associated with the time-varying electron density irregularity in the midlatitude region. Additionally, we analyzed the spatial scale of the observed EMIC waves and their contribution to the thermal ion heating.

1. Introduction

Fine-structured electromagnetic ion cyclotron (EMIC) waves are one type of EMIC mode waves, and ground-based Pc1 studies have reported that they are composed of clear repetitive bursts of characteristic rising tones in a typical frequency range of 0.2–5 Hz (Fukunishi et al., 1981; Troitskaya & Gul'elmi, 1967). Multipoint measurement of fine-structured EMIC waves reveals their propagation mechanism, formation mechanism, and wave-particle interaction along their propagation path. For example, Usanova et al. (2008) presented simultaneous ground-satellite observations of fine-structured EMIC waves and reported that the repetition periods of fine-structured EMIC waves observed on the ground and on the Time History of Events and Macroscale Interactions During Substorms (THEMIS) spacecraft were almost identical. They concluded that these observation results cannot be explained by the bouncing wave packet (BWP) model

© 2021. The Authors.

This is an open access article under the terms of the [Creative Commons Attribution-NonCommercial-NoDerivs License](https://creativecommons.org/licenses/by/4.0/), which permits use and distribution in any medium, provided the original work is properly cited, the use is non-commercial and no modifications or adaptations are made.

Resources: S. Matsuda, Y. Miyoshi, Y. Kasahara, K. Asamura, Y. Kasaba, A. Matsuoka, F. Tsuchiya, A. Kumamoto, S. Nakamura, M. Kitahara, I. Shinohara, G. Reeves, H. Spence, K. Shiokawa, T. Nagatsuma, S. Oyama, I. R. Mann
Software: S. Matsuda
Supervision: S. Matsuda, Y. Miyoshi, Y. Kasahara
Validation: S. Matsuda, Y. Miyoshi, Y. Kasahara, L. Blum, C. Colpitts, K. Asamura, Y. Kasaba, A. Matsuoka, F. Tsuchiya, A. Kumamoto, M. Teramoto, S. Nakamura, M. Kitahara, I. Shinohara, G. Reeves, H. Spence, K. Shiokawa, T. Nagatsuma, S. Oyama, I. R. Mann
Visualization: S. Matsuda
Writing – original draft: S. Matsuda
Writing – review & editing: S. Matsuda, Y. Miyoshi, Y. Kasahara, L. Blum, C. Colpitts, K. Asamura, Y. Kasaba, A. Matsuoka, F. Tsuchiya, A. Kumamoto, M. Teramoto, S. Nakamura, M. Kitahara, I. Shinohara, G. Reeves, H. Spence, K. Shiokawa, T. Nagatsuma, S. Oyama, I. R. Mann

proposed by Jacobs and Watanabe (1964) and Obayashi (1965). Similar questions about the BWP model were raised by Erlandson and Anderson (1996) and Mursula et al. (2001).

Several recent studies have examined the role of fine-structured EMIC waves from the perspective of wave-particle interaction. Sakaguchi et al. (2015) and Nomura et al. (2016) found that fine-structured EMIC waves cause isolated proton auroras (IPAs). This is evidence that fine-structured EMIC waves scatter energetic protons, which then precipitate into the ionosphere. Ozaki et al. (2018) reported 1 Hz range modulation of IPAs and concluded that the modulation was due to intermittent proton precipitation or sub-relativistic electrons scattered by repetitive bursts of fine-structured EMIC waves. EMIC waves that cause IPA work for MeV electron scattering (e.g., Miyoshi et al., 2008) and the density irregularity of the topside ionosphere (Kim et al., 2021).

In this study, we present the results of the coordinated observation of fine-structured EMIC waves on April 18, 2019 by Arase (midlatitude region), Van Allen Probe A (Radiation Belt Storm Probes A, hereinafter called RBSP-A) (equatorial region), and induction magnetometers placed on the Gakona station of the “study of dynamical variation of Particles and Waves in the INner magnetosphere using Ground-based network observations” (PWING) magnetometer and the Dawson station of the “Canadian Array for Realtime Investigations of Magnetic Activity” (CARISMA) magnetometer array. We report that the growth of the observed fine-structured EMIC waves was associated with the periodic electron density irregularities found in the midlatitude region. Further, we investigate the differences in the wave properties of fine-structured EMIC waves observed in each latitude, and the thermal ion heating due to fine-structured EMIC waves, using observations from these four sites.

2. Data

We used the level-2 electric and magnetic field waveforms observed by the Electric Field Detector (EFD) (Kasaba et al., 2017; Kasahara et al., 2020; Kasahara, Kasaba, et al., 2018) and the Magnetic Field Experiment (MGF) (Matsuoka, Teramoto, Imajo, et al., 2018; Matsuoka, Teramoto, Nomura, et al., 2018) aboard Arase (Miyoshi, Shinohara, Takashima, et al., 2018) for the EMIC wave analysis. To determine the ambient electron density from the upper hybrid resonance (UHR) frequencies, we used the level-2 electric field spectrum data observed by the High Frequency Analyzer (HFA) (Kasahara, Kumamoto, et al., 2018; Kumamoto et al., 2018).

The low-energy particle experiments-ion mass analyzer (LEP-i) (Asamura, Kazama, et al., 2018) measures ions with an energy range from 0.01 to 25 keV/q. We used the level-2 three-dimensional proton flux data (Asamura, Miyoshi, & Shinohara, 2018) to analyze the energy-time diagrams, and the level-3 pitch-angle distribution data (Asamura et al., 2021). In addition, we used the DC magnetic field data measured by the MGF to calculate the ion cyclotron frequencies and the ambient magnetic field direction. We also used the level-2 definitive orbit data of Arase (Miyoshi, Shinohara, & Jun, 2018).

The Electric and Magnetic Field Instrument and Integrated Science (EMFISIS) aboard the RBSP measures three components of the electric field and three components of the magnetic field below 12 kHz (Kletzing et al., 2013). The ambient magnetic field is also measured by the magnetometer of EMFISIS. In this study, we used the high-resolution (64 samples per second) level-3 DC magnetic field vector data in the solar magnetic coordinate system.

The Helium Oxygen Proton Electron mass spectrometer instrument (HOPE) is a subsystem of the Energetic Particle Composition and Thermal Plasma Suite (ECT) instrument aboard RBSP. HOPE measures electrons, protons, helium ions, and oxygen ions with energies from 20 eV to 45 keV (Funsten et al., 2013; Spence et al., 2013). We used the level-2 proton flux data and level-3 pitch-angle distribution data.

We used the induction magnetometer data from the Gakona station (62.39°N and 145.15°W geographic coordinates) of the PWING magnetometer (Shiokawa et al., 2017), and the Dawson station (64.048°N and 139.11°W geographic coordinates) of the CARISMA magnetometer array (Mann et al., 2008). These two stations are separated by ~350 km. The sampling frequencies of the data are 64 and 2 Hz for the Gakona and Dawson stations, respectively.

3. Observation

Figures 1a–1e display the results of simultaneous plasma wave observations from 00:40 to 02:40 UT on April 18, 2019 by the Arase/PWE-HFA, PWE-EFD, MGF, RBSP-A/EMFISIS-HFR, EMFISIS magnetometer, induction magnetometers located at the Gakona and Dawson stations, respectively. The frequency resolution of the short-time Fourier transform analysis was 7.8125 mHz. The black dashed lines in Figures 1b and 1c indicate the local oxygen ion cyclotron frequencies (F_{O^+}) derived from the DC magnetic field measurement by Arase/MGF. The black solid line in Figure 1e indicates the local helium ion cyclotron frequencies (F_{He^+}) derived from the DC magnetic field measured by the EMFISIS magnetometer aboard RBSP-A. The electric field measurement by the RBSP-A/EFW is not presented here because the data quality was insufficient owing to instrument degradation. Figures 1h–1j present the McIlwain- L values derived from the T89 model (Tsyganenko, 1989), the magnetic latitudes, and the magnetic local times of both satellites (red: Arase, blue: RBSP-A). Arase and RBSP-A were orbiting at almost the same magnetic local time (15.4 hr) and the same L -shell ($L = 5.7$) at 01:34 UT (the vertical dash-dotted line in Figure 1). The magnetic latitude of Arase was $\sim 28^\circ$, whereas RBSP-A was near the geomagnetic equatorial region. The Dst index was ~ 5 nT, and the Kp index was 0 during the event, indicating quiet conditions. According to the magnetic field measurements by Arase/MGF and RBSP-A/EMFISIS, no Pc3–Pc5 range ULF wave activity was detected during this period.

As illustrated in Figures 1a–1c, fine-structured EMIC waves in helium band were observed in the two frequency ranges of 0.40–0.53 Hz and 0.50–0.66 Hz by Arase (outside of plasmopause). The former was observed from 01:17 to 01:38 UT and the latter was observed from 01:31 to 01:47 UT. The maximum amplitude of these EMIC waves was ~ 0.7 nT. It is evident that some rising-tone elements are embedded in these EMIC waves, and the repetition of these rising-tones clearly corresponds (red vertical lines) to the periodic changes of the electric field spectra near the UHR emission visible in the higher frequency electric field spectra (Figure 1a).

In Figure 1a, the black line shows the UHR frequency (f_{UHR}) determined by the combination of the automatic cutoff frequency detection and visual inspection from the observed UHR emission (Kumamoto et al., 2018). The white lines at the top and middle show the electron plasma frequency (f_p) and the Z-mode cutoff frequency (f_z). The purple dashed lines at the top and bottom show $5f_c$ and $4f_c$, respectively. Here, f_c denotes the local electron cyclotron frequency derived from the DC magnetic field measurement by Arase/MGF. Figure 1a indicates that the discrete and intermittent emissions in the frequency range below UHR emission were Z-mode waves. Although the variation in UHR frequency was not clear, owing to the limited time and frequency resolutions of the HFA, we have concluded that there were some density irregularities along the orbit of Arase (see also Barnhart et al., 2009). The ambient electron density variation derived from the observed UHR emission is shown as the bottom white line in Figure 1a. The gray dashed lines show the upper and lower envelopes of the derived electron density variation. The averaged time duration and interval of observed density irregularities were approximately 25 and 145 s, respectively. The averaged spatial extent and separation were approximately $0.01R_E$ and $0.05R_E$, respectively, where R_E denotes Earth radii. See also Figures S1a–S1c for an enlarged view of the Arase observation.

As illustrated in Figures 1d–1g, fine-structured EMIC waves were observed in almost the same frequency ranges at the equatorial region (RBSP-A) and the Gakona and Dawson stations. The frequency-time spectra of the observed EMIC waves in the equatorial region and the Gakona and Dawson stations were quite similar during the entire event (01:20–02:30 UT). However, the lower-frequency EMIC wave (0.40–0.53 Hz, 01:35–01:50 UT) observed by RBSP-A was weaker than those observed by Arase and the two ground stations in the same frequency range. Simultaneous observations of EMIC waves in almost the same frequency range were successfully performed from 01:17 to 01:47 UT by Arase, RBSP-A and the two ground stations. During this time interval, Arase and RBSP-A were at almost the same magnetic local time (15.4 hr) and the same L -shell region ($L = 5.26$ – 6.30 and 5.70 – 5.82 for Arase and RBSP-A, respectively), but in different magnetic latitude regions (28.8° and -0.8° for Arase and RBSP-A, respectively). Although RBSP-A passed through the L -shell region of 5.70 – 5.82 , there were no density irregularities, like those observed by Arase/PWE-HFA in the UHR frequency variation, seen in the equatorial region by RBSP-A/EMFISIS-HFR. The EMIC wave power spectral density in the midlatitude region (Arase) was significantly larger than that in the equatorial region (RBSP-A) around the field line conjunction interval. The wave amplitudes observed at the two ground stations (Gakona and Dawson) were smaller than those from Arase by 1–2 orders of magnitude.

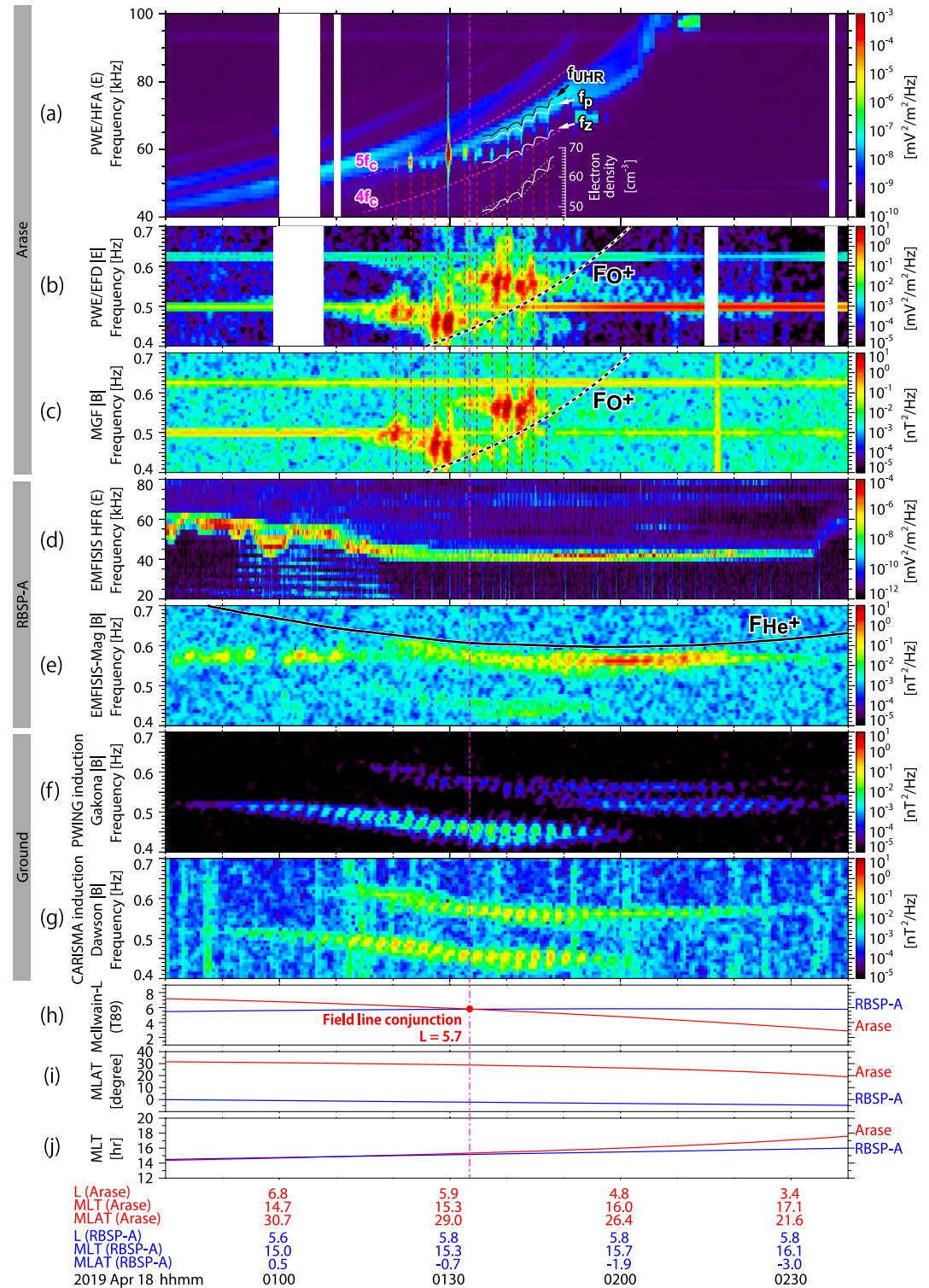


Figure 1. Dynamic wave-power spectra from 00:40–02:40 UT on April 18, 2019 observed by (a) Arase/PWE-High Frequency Analyzer (HFA), (b) Arase/PWE-Electric Field Detector (EFD), (c) Arase/Magnetic Field Experiment (MGF), (d) Radiation Belt Storm Probes A (RBSP-A)/Electric and Magnetic Field Instrument and Integrated Science (EMFISIS)-HFR, (e) RBSP-A/EMFISIS magnetometer, (f) induction magnetometer located at the Gakona station, (g) induction magnetometer located at the Dawson station. (h) McIlwain- L values calculated from the T89 model, (i) magnetic latitudes, and (j) magnetic local times of Arase (red) and RBSP-A (blue).

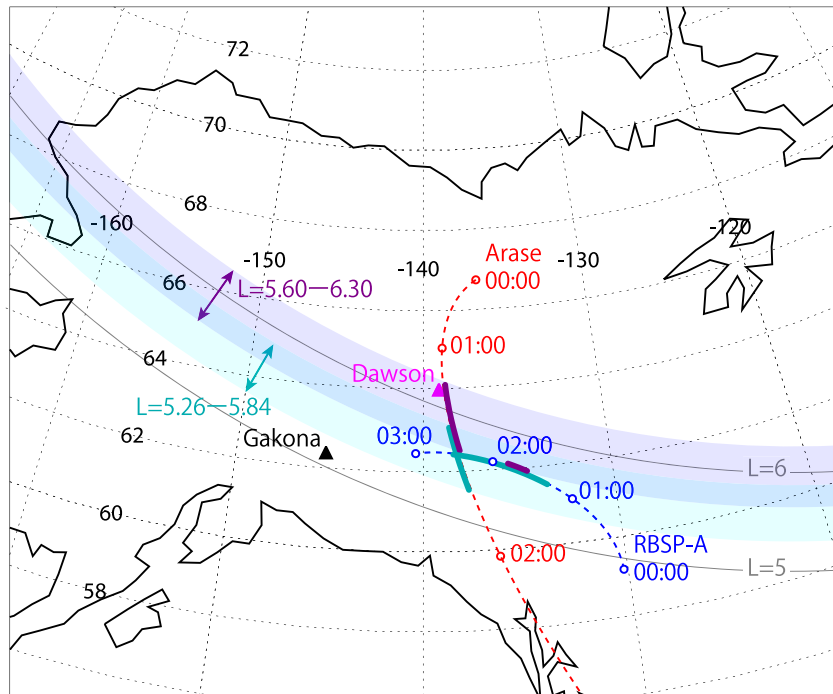


Figure 2. Magnetic footprint of Arase (red) and Radiation Belt Storm Probes A (RBSP-A) (blue) at the altitude of the ionosphere (100 km) for the time interval of 00:00–03:00 UT on April 18, 2019.

The averaged repetition periods of the fine structures observed by Arase, RBSP-A, and two ground stations were ~ 140 s regardless of the measurement location. This is comparable to the averaged repetition period of the density irregularities observed by Arase (~ 145 s). These repetition periods were derived by visual inspection; therefore, the results should contain errors on the order of seconds.

Figure 2 presents the magnetic footprint of Arase (red) and RBSP-A (blue) at the altitude of the ionosphere (100 km) for the time interval from 00:00 to 03:00 UT on April 18, 2019. Arase was orbiting from north to south during this period ($66.7\text{--}35.4^\circ\text{N}$ and $136.7\text{--}112.3^\circ\text{W}$ geographic coordinates) and passed by the Dawson station (magenta triangle at 64.048° in latitude) at 01:18 UT. In contrast, RBSP-A was orbiting from east to west during this period ($59.2\text{--}62.5^\circ\text{N}$ and $130.2\text{--}140.4^\circ\text{W}$ geographic coordinates). The location of the Gakona station is represented as a black triangle. The bold purple and light blue lines indicate the locations where lower-frequency EMIC waves (0.40–0.53 Hz) were observed and the higher-frequency EMIC waves (0.50–0.66 Hz) were observed by each satellite, respectively. The purple and light blue shaded regions denote the L -shell regions where the lower and higher frequency EMIC waves were observed, respectively. Both lower- and higher-frequency EMIC waves were observed in the overlapping region, where $L = 5.60\text{--}5.84$. By comparing the observations by Arase and RBSP-A, it was found that both EMIC waves were confined to narrow L -shell ranges. Because the trajectory of RBSP-A was traversing the edge of the overlapping region, a weak lower-frequency EMIC wave was observed from 01:35 to 01:50 UT by RBSP-A, as shown in Figure 1e.

Figures 3a–3d present thermal ion observations on RBSP-A from 00:00 to 03:00 UT on April 18, 2019. Figure 3a displays the magnetic field spectra observed by EMFISIS. Figures 3c and 3d display the pitch-angle distributions of H^+ and He^+ for the energy range of 2–98 eV observed by ECT/HOPE. As illustrated in Figures 3c and 3d, two clear signatures of thermal ion enhancement corresponding to the EMIC wave activity were observed: the enhancement of thermal protons with pitch-angles of $9\text{--}27^\circ$ and $153\text{--}171^\circ$ from 00:51 to 01:25 UT, and that of thermal He^+ with pitch-angles of $45\text{--}135^\circ$ from 01:50 to 02:18 UT. The enhancement of H^+ with pitch-angles of $9\text{--}27^\circ$ and $153\text{--}171^\circ$ was observed in a limited time within the interval of EMIC waves that does not correspond to any enhancement in wave activity. On the other hand, the enhancement of He^+ clearly corresponded to a period of enhanced EMIC wave intensity ($L = 5.75\text{--}5.77$). This He^+ enhancement was not observed by Arase (not shown here).

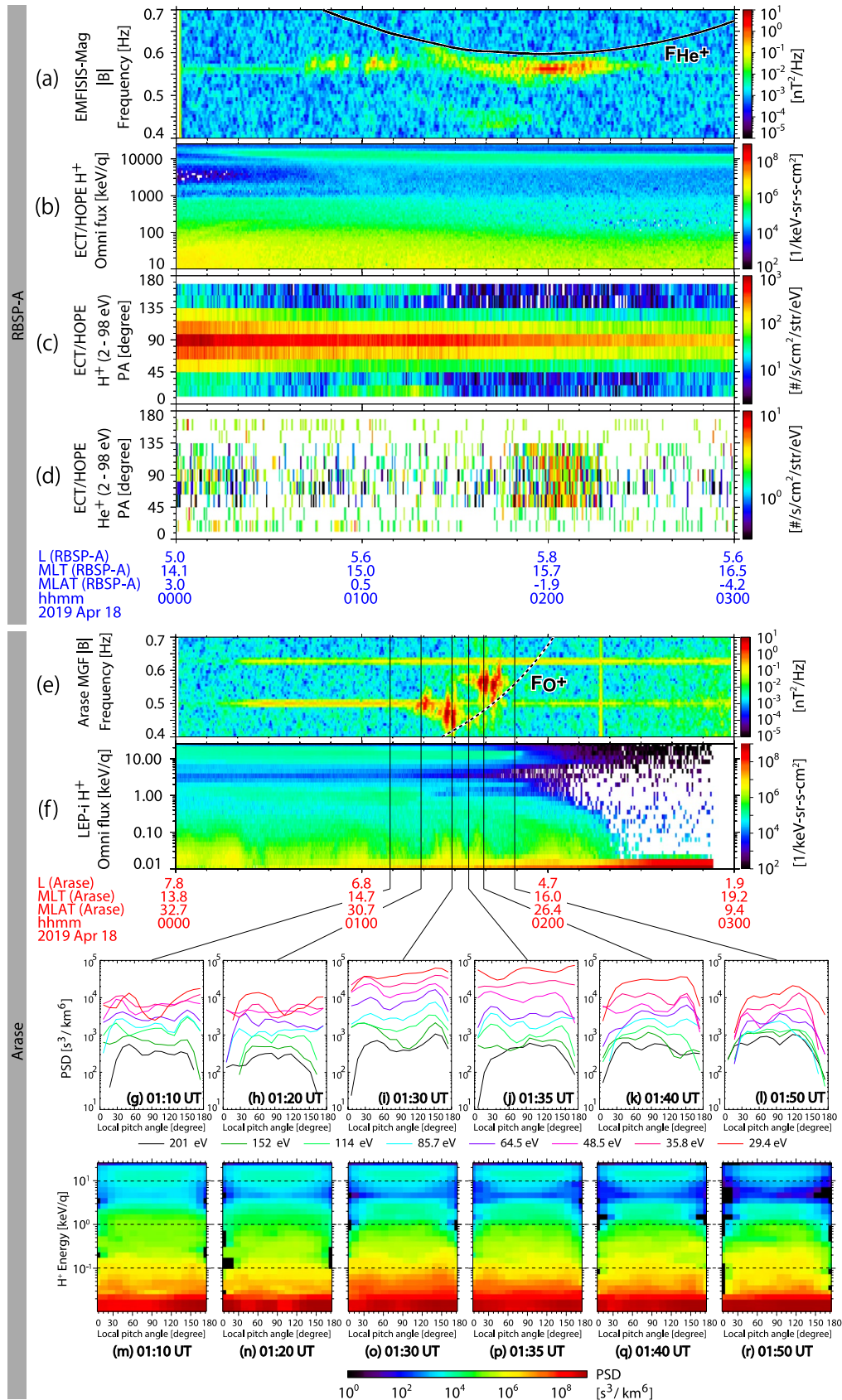


Figure 3.

Figures 3g–3r display the phase-space densities (PSD) of protons as a function of the local pitch-angle observed by Arase/LEP-i at 01:10 UT (before the EMIC waves were observed), 01:20 UT, 01:30 UT, 01:35 UT, 01:40 UT (while the EMIC waves were observed), and 01:50 UT (after the EMIC waves were observed) on April 18, 2019. The corresponding wave spectra observed by the Arase/MGF are shown in Figure 3e. Note that we used data from 5 min before and after the time of interest when we calculate the proton pitch-angle distributions. As illustrated in Figures 3i–3k and 3o–3g, clear signatures of less than 200 eV/q proton heating with local pitch-angles around 30° and 150° were observed in the interval from 01:30 to 01:40 UT ($L = 5.87$ – 5.52).

The corresponding measurements of the omnidirectional proton fluxes by Arase/LEP-i and RBSP-A/ECT-HOPE are displayed in Figures 3b and 3f. Both Arase and RBSP-A detect ion nose structures near the inner edge of the duskside plasma sheet (e.g., Ren et al., 2021), and no periodic changes were observed in the proton distribution during the interval of the fine-structured EMIC wave activity.

4. Discussion

4.1. EMIC Wave Growth Near the Density Irregularities

We found that the modulation of the observed EMIC waves clearly corresponded to the lower cutoff frequency variation of the electric field spectra near the UHR emission observed by Arase. If we assume that this indicates variation in the Z-mode cutoff frequency, we can derive the ambient electron density along the orbit of Arase (Barnhart et al., 2009). According to the electric field measurement by Arase/PWE-HFA, the maximum change in the electron density was ~8%, while the averaged change was ~5%. Note that the frequency resolution of EMFISIS-HFR is ~2.1 kHz in the frequency range of observed UHR emission; thus, small density changes less than 10% cannot be detected by RBSP-A. The RBSP-A measurement suggests that there are no density irregularities of larger than 10% in the equatorial region, however, the possibility of the existence of small-scale density irregularities of less than 10% remains. Because the spatial extent of these density irregularities is unclear, the question on the wave guiding along the density irregularities is still open. On the other hand, we discuss the scale of wave propagation duct estimated from the multipoint wave measurement in Section 4.2.

A ray tracing study done by de Soria-Santacruz et al. (2013) reproduced cold plasma density irregularities using an analytical model and showed that the cold plasma irregularities with 20% density variations between $L = 5$ and $L = 7$ can cause periodic growth of He⁺ band EMIC waves. Further, they also showed that the density irregularities are responsible for a guide of the wave propagation along the ducts. The conditions used in their ray tracing study were similar to the conditions during the fine-structured EMIC wave event presented in this study. The density variations of the irregularities observed by Arase were at most 8% and smaller than the irregularity assumed by de Soria-Santacruz et al. (2013). Moreover, Yue et al. (2020) showed the observation of intermittent EMIC waves associated to the clear density cavities along the orbit of RBSP-B. The scale of density cavities shown by Yue et al. (2020) (~60% density changes, several minutes order) is much larger than our present observation. We need to investigate how the different-scale density irregularities contribute to the EMIC wave growth in future studies.

Arase crossed the L -shell region from 5.35 to 6.20 during the event; thus, the observed periodic changes in the Z-mode cutoff frequency can be explained by the presence of radial cold plasma density irregularities as one possibility (spatially varying). Alternatively, it can also be explained as periodic changes in electron density at a given location (time-varying). By comparing the EMIC wave spectra observed by Arase and RBSP-A, the periods of the observed fine structures by both satellites were almost the same. Note that RBSP-A was orbiting at an almost fixed L -shell ($L = 5.8$) during the event. Assuming that the fine-structure of

Figure 3. Summary of thermal ion observations from 00:00 to 03:00 UT on April 18, 2019. (a) Dynamic wave-power spectra observed by Radiation Belt Storm Probes A (RBSP-A)/Electric and Magnetic Field Instrument and Integrated Science (EMFISIS), (b–d) omnidirectional H⁺ fluxes and pitch-angle distributions of H⁺ and He⁺ for 2–98 eV ions observed by RBSP-A/Energetic Particle Composition and Thermal Plasma Suite (ECT)-Helium Oxygen Proton Electron mass spectrometer instrument (HOPE), (e) dynamic wave-power spectra observed by Arase/Magnetic Field Experiment (MGF), (f) omnidirectional H⁺ fluxes, and (g–r) time variation of the phase space density of H⁺ as a function of the local pitch-angle observed by Arase/low-energy particle experiments-ion mass analyzer (LEP-i).

observed EMIC waves was caused by the steep radial variation in electron density, RBSP-A should measure the fine-structured EMIC waves with a significantly larger periodicity than that observed by Arase. Additionally, if we assume duct propagation along the density irregularities, this implies that the irregularity repeatedly occurred on the same field line. Hence, we conclude the observed electron density irregularities were caused by time-varying electron density changes.

As mentioned in Section 3, the wave power spectral density in the midlatitude region was significantly larger than that in the equatorial region. This result suggests the EMIC wave growth associated with the density irregularities observed in the midlatitude region, and supports midlatitude source EMIC waves reported by Vines et al. (2019). Matsuda et al. (2018) conducted a statistical study of fine-structured EMIC waves using the data obtained by Arase for 12 months and found that the dominant region of the fine-structured EMIC waves is the midlatitude region ($10^\circ < |\text{MLAT}| < 30^\circ$). The EMIC event in this study was observed on Arase at magnetic latitude around 28° ; therefore, it is consistent with their statistical result. We need to clarify the generation mechanism of other fine-structured EMIC waves in the midlatitude region reported by Matsuda et al. (2018) as a next step.

4.2. Spatial Extent of the Observed EMIC Waves

Multipoint measurement can be a powerful tool for revealing the spatial extent of plasma waves in the magnetosphere. As summarized in Figure 2, the lower and higher frequency EMIC waves discussed in this study were observed at limited L -shell ranges of 5.60–6.30 ($\Delta L = 0.7$) and 5.26–5.84 ($\Delta L = 0.58$), respectively. Here ΔL denotes the size of a limited L -shell region. Using the T89 magnetic field model, both these narrow L -shell ranges correspond to ~ 185 km latitudinal width at an auroral altitude of 100 km.

Focusing on the frequency bandwidths of the EMIC waves observed by Arase and RBSP-A, they are almost the same (~ 0.08 Hz) around the timing of the field line conjunction (Arase & RBSP-A: $L = 5.7$, 01:34 UT). On the other hand, before 01:30 UT (Arase: $L > 5.8$) and after 01:38 UT (Arase: $L < 5.5$), the frequency bandwidth of the EMIC waves observed by Arase is broader than the RBSP-A result. Because these broadband EMIC waves were not observed by RBSP-A and two ground stations, we concluded that the spatial scale of the wave propagation duct was approximately less than 80 km ($\Delta L < 0.3$) at an auroral altitude of 100 km. This scale is smaller than the EMIC wave activity region (~ 185 km) estimated from the both Arase and RBSP-A observations.

Sakaguchi et al. (2015) showed a comprehensive study of the spatial extent of IPAs using all-sky imagers located in Athabasca. Their statistical analysis showed that the latitudinal width of proton auroral arcs due to pitch-angle scattering caused by EMIC waves was typically from 30 to 120 km at ionospheric altitudes, and has a clear peak at ~ 56 km. The estimated latitudinal width of the propagation duct at an auroral altitude of 100 km shown in this study is consistent with their statistical result, suggesting that IPAs are a visual manifest of wave-particle interaction regions.

4.3. Thermal Ion Heating by EMIC Waves

As shown in Section 3, the enhancement of He^+ with pitch-angles of $45\text{--}135^\circ$ observed by RBSP-A clearly corresponds to the timing of the enhancement of EMIC wave intensity ($L = 5.75\text{--}5.77$). Considering the conservation of the first adiabatic invariant as well as the total energy, ions with a pitch-angle of more than 35° at the geomagnetic equator do not reach the magnetic latitude of Arase. Anderson and Fuselier (1994) and Fuselier and Anderson (1996) discussed the mechanism of perpendicular He^+ heating by EMIC waves due to cyclotron resonance interactions. There have been several observations on perpendicular thermal He^+ heating by EMIC waves near the helium gyrofrequency (e.g., Zhang et al., 2011 and references therein). The present observations show clear perpendicular He^+ heating which coincided with the appearance of the intense EMIC wave just below the helium gyrofrequency (Figures 3a and 3d), and is consistent with previous studies.

RBSP-A measured a clear enhancement of H^+ with pitch-angles of $9\text{--}27^\circ$ and $153\text{--}171^\circ$ at $L = 5.55\text{--}5.71$, and Arase also measured H^+ with pitch-angles of 30° and 150° in almost the same L -shell region ($L = 5.87\text{--}5.52$). The local-pitch angle of 30° at the location of Arase corresponds to 17° equatorial pitch-angle; therefore,

we conclude that both Arase and RBSP-A measured the same enhanced ion distribution within a narrow L -shell range. Considering the time lag between these two measurements, this H^+ enhancement is present steadily for at least several tens of minutes. RBSP-A observed a proton enhancement within the EMIC wave active interval, which did not correspond to any variation in EMIC wave intensity. On the other hand, the enhancement clearly coincided with the EMIC waves observed by Arase. This evidence suggests that the observed H^+ enhancement may have occurred in the midlatitude region, rather than the equatorial region. A similar enhancement of thermal protons corresponding to EMIC wave activity was reported by Ma et al. (2019); however, the mechanism of thermal proton heating due to fine-structured EMIC waves is still unclear. Omura et al. (1988) suggest that parallel heating is associated with the interaction of forward and backward propagating EMIC waves. Further study is necessary to clarify the contribution of fine-structured EMIC waves to proton heating.

5. Summary

In this study, we discussed the properties of the observed fine-structured EMIC waves using a multipoint conjunction event. The results are summarized as follows:

1. We successfully measured latitudinally propagating EMIC waves by Arase and RBSP-A on April 18, 2019. These EMIC waves were also observed at the Gakona and Dawson ground stations.
2. Nearly identical EMIC wave spectra were observed by Arase, RBSP-A, and the two ground stations within a limited time interval. By comparing the footprints and wave spectra of both satellites, we concluded that the observed EMIC wave activity was spatially localized (185 km latitudinal width at an auroral altitude of 100 km) and the spatial scale of the wave propagation duct was smaller (<80 km) than the EMIC wave activity region.
3. We found that the periodicity of the fine-structured EMIC waves observed by Arase coincided with the time-varying electron density irregularities. These density irregularities should be responsible for the EMIC wave growth as demonstrated by de Soria-Santacruz et al. (2013).
4. Thermal He^+ heating was observed coincident with fine-structured EMIC waves. Additionally, the clear heating of protons with local pitch-angles of approximately 30° and 150° was detected by Arase concurrently with the appearance of fine-structured EMIC waves. This thermal ion distribution was also observed in the equatorial region by ECT/HOPE aboard RBSP-A.

Data Availability Statement

Science data of the ERG (Arase) satellite were obtained from the ERG Science Center operated by ISAS/JAXA and ISEE/Nagoya University (Miyoshi, Hori, et al., 2018) (<https://ergsc.isee.nagoya-u.ac.jp/index.shtml.en>). In the present study, we used level-2 PWE/EFD 64 Hz waveform v01.01 data (Kasahara et al., 2020), level-2 MGF 64 Hz waveform v03.04 data (Matsuoka, Teramoto, Imajo, et al., 2018), level-2 PWE/HFA spectrum data v01.02 data (Kasahara, Kumamoto, et al., 2018), level-2 LEP-i 3D flux v03.00 data (Asamura, Miyoshi, & Shinohara, 2018), level-3 LEP-i pitch angle sorted data (Asamura et al., 2021), and level-2 definitive orbit v03 data (Miyoshi, Shinohara, & Jun, 2018). Dst and Kp indices data used in this study was provided by the “Geospatial Information Authority of Japan” and “WDC for Geomagnetism, Kyoto” (<http://wdc.kugi.kyoto-u.ac.jp/wdc/Sec3.html>). The EMFISIS data and ECT data are obtained from <https://emfisis.physics.uiowa.edu/data/index/> and <http://www.RBSP-ect.lanl.gov>. The PWING magnetometer data are obtained from <https://stdb2.isee.nagoya-u.ac.jp/magne/>. The CARISMA data are obtained from <https://www.carisma.ca>. The SPEDAS software (Angelopoulos et al., 2019) was used for the data analysis in this study.

References

- Anderson, B. J., & Fuselier, S. A. (1994). Response of thermal ions to electromagnetic ion cyclotron waves. *Journal of Geophysical Research*, 99(A10), 19413–19425. <https://doi.org/10.1029/94ja01235>
- Angelopoulos, V., Cruce, P., Drozdov, A., Grimes, E. W., Hatzigeorgiou, N., King, D. A., et al. (2019). The space physics environment data analysis system (SPEDAS). *Space Science Reviews*, 215(1), 9. <https://doi.org/10.1007/s11214-018-0576-4>
- Asamura, K., Kazama, Y., Yokota, S., Kasahara, S., & Miyoshi, Y. (2018). Low-energy particle experiments—ion mass analyzer (LEPI) on-board the ERG (ARASE) satellite. *Earth, Planets and Space*, 70(1), 70. <https://doi.org/10.1186/s40623-018-0846-0>

Acknowledgments

The authors wish to acknowledge the EMFISIS and ECT team for providing data. The authors thank D. K. Milling and the rest of the CARISMA team for providing data. CARISMA is operated by the University of Alberta, funded by the Canadian Space Agency. The authors acknowledge the International Space Sciences Institute (ISSI) and the participants in a 2020 ISSI workshop in Bern on “Radiation belt physics from top to bottom.” Part of this work was done at the ERG-Science Center operated by ISAS/JAXA and ISEE/Nagoya University. This study was supported by Grants-in-Aid for Scientific Research (14J02108, 16H06286, 17H06140, 20K14546, and 20H01959) of Japan Society for the Promotion of Science (JSPS). This study was supported by JSPS Bilateral Open Partnership Joint Research Projects (JPJSBP120192504).

- Asamura, K., Miyoshi, Y., Matsuoka, A., Teramoto, M., & Shinohara, I. (2021). *The LEPI instrument level-3 pitch angle distribution (PAD) flux data of exploration of energization and radiation in geospace (ERG) ARASE satellite* (Version v03.00, updated daily). ERG Science Center, Institute for Space-Earth Environmental Research, Nagoya University. <https://doi.org/10.34515/DATA.ERG-05002>
- Asamura, K., Miyoshi, Y., & Shinohara, I. (2018). *The LEPI instrument level-2 3D flux data of exploration of energization and radiation in geospace (ERG) ARASE satellite* (Version v01.00, updated daily). ERG Science Center, Institute for Space-Earth Environmental Research, Nagoya University. <https://doi.org/10.34515/DATA.ERG-05000>
- Barnhart, B. L., Kurth, W. S., Groene, J. B., Faden, J. B., Santolik, O., & Gurnett, D. A. (2009). Electron densities in Jupiter's outer magnetosphere determined from voyager 1 and 2 plasma wave spectra. *Journal of Geophysical Research*, *114*(A5). <https://doi.org/10.1029/2009ja014069>
- de Soria-Santacruz, M., Spasojevic, M., & Chen, L. (2013). EMIC waves growth and guiding in the presence of cold plasma density irregularities. *Geophysical Research Letters*, *40*(10), 1940–1944. <https://doi.org/10.1002/grl.50484>
- Erlanson, R. E., & Anderson, B. J. (1996). Pc 1 waves in the ionosphere: A statistical study. *Journal of Geophysical Research*, *101*(A4), 7843–7857. <https://doi.org/10.1029/96ja00082>
- Fukunishi, H., Toya, T., Koike, K., Kuwashima, M., & Kawamura, M. (1981). Classification of hydromagnetic emissions based on frequency-time spectra. *Journal of Geophysical Research*, *86*(A11), 9029–9039. <https://doi.org/10.1029/ja086a11p09029>
- Funsten, H. O., Skoug, R. M., Guthrie, A. A., MacDonald, E. A., Baldonado, J. R., Harper, R. W., et al. (2013). Helium, oxygen, proton, and electron (HOPE) mass spectrometer for the radiation belt storm probes mission. *Space Science Reviews*, *179*(1), 423–484. <https://doi.org/10.1007/s11214-013-9968-7>
- Fuselier, S. A., & Anderson, B. J. (1996). Low-energy He⁺ and H⁺ distributions and proton cyclotron waves in the afternoon equatorial magnetosphere. *Journal of Geophysical Research*, *101*(A6), 13255–13265. <https://doi.org/10.1029/96ja00292>
- Jacobs, J., & Watanabe, T. (1964). Micropulsation whistlers. *Journal of Atmospheric and Terrestrial Physics*, *26*(8), 825–829. [https://doi.org/10.1016/0021-9169\(64\)90180-1](https://doi.org/10.1016/0021-9169(64)90180-1)
- Kasaba, Y., Ishisaka, K., Kasahara, Y., Imachi, T., Yagitani, S., Kojima, H., et al. (2017). Wire probe antenna (WPT) and electric field detector (EFD) of plasma wave experiment (PWE) aboard the ARASE satellite: Specifications and initial evaluation results. *Earth, Planets and Space*, *69*(1), 174. <https://doi.org/10.1186/s40623-017-0760-x>
- Kasahara, Y., Kasaba, Y., Kojima, H., Yagitani, S., Ishisaka, K., Kumamoto, A., et al. (2018). The plasma wave experiment (PWE) on board the ARASE (ERG) satellite. *Earth, Planets and Space*, *70*(1), 86. <https://doi.org/10.1186/s40623-018-0842-4>
- Kasahara, Y., Kasaba, Y., Matsuda, S., Shoji, M., Nakagawa, T., Ishisaka, K., et al. (2020). *The PWE/EFD instrument level-2 electric field waveform data of exploration of energization and radiation in geospace (ERG) ARASE satellite* (Version v01.01, updated daily). ERG Science Center, Institute for Space-Earth Environmental Research, Nagoya University. <https://doi.org/10.34515/DATA.ERG-07003>
- Kasahara, Y., Kumamoto, A., Tsuchiya, F., Matsuda, S., Shoji, M., Nakamura, S., et al. (2018). *The PWE/HFA instrument level-2 spectrum data of exploration of energization and radiation in geospace (ERG) ARASE satellite* (Version v01.02, updated daily). ERG Science Center, Institute for Space-Earth Environmental Research, Nagoya University. <https://doi.org/10.34515/DATA.ERG-10000>
- Kim, H., Shiokawa, K., Park, J., Miyoshi, Y., Miyashita, Y., Stolle, C., et al. (2021). Isolated proton aurora driven by EMIC PC1 wave: PWING, swarm, and NOAA POES multi-instrument observations. *Geophysical Research Letters*, *48*(18), e2021GL095090. <https://doi.org/10.1029/2021gl095090>
- Kletzing, C. A., Kurth, W. S., Acuna, M., MacDowall, R. J., Torbert, R. B., Averkamp, T., et al. (2013). The electric and magnetic field instrument suite and integrated science (EMFISIS) on RBSP. *Space Science Reviews*, *179*(1), 127–181. <https://doi.org/10.1007/s11214-013-9993-6>
- Kumamoto, A., Tsuchiya, F., Kasahara, Y., Kasaba, Y., Kojima, H., Yagitani, S., et al. (2018). High frequency analyzer (HFA) of plasma wave experiment (PWE) onboard the ARASE spacecraft. *Earth, Planets and Space*, *70*(1), 82. <https://doi.org/10.1186/s40623-018-0854-0>
- Ma, Q., Li, W., Yue, C., Thorne, R. M., Bortnik, J., Kletzing, C. A., et al. (2019). Ion heating by electromagnetic ion cyclotron waves and magnetosonic waves in the earth's inner magnetosphere. *Geophysical Research Letters*, *46*(12), 6258–6267. <https://doi.org/10.1029/2019gl083513>
- Mann, I. R., Milling, D. K., Rae, I. J., Ozeke, L. G., Kale, A., Kale, Z. C., et al. (2008). The upgraded carisma magnetometer array in the themis era. In J. L. Burch, & V. Angelopoulos (Eds.), *The themis mission* (pp. 413–451). Springer New York. https://doi.org/10.1007/978-0-387-89820-9_18
- Matsuda, S., Kasahara, Y., Miyoshi, Y., Nomura, R., Shoji, M., Matsuoka, A., et al. (2018). Spatial distribution of fine-structured and unstructured EMIC waves observed by the ARASE satellite. *Geophysical Research Letters*, *45*(21), 11530–11538. <https://doi.org/10.1029/2018gl080109>
- Matsuoka, A., Teramoto, M., Imajo, S., Kurita, S., Miyoshi, Y., & Shinohara, I. (2018). *The MGF instrument level-2 high-resolution magnetic field data of exploration of energization and radiation in geospace (ERG) ARASE satellite* (Version v03.04, updated daily). ERG Science Center, Institute for Space-Earth Environmental Research, Nagoya University. <https://doi.org/10.34515/DATA.ERG-06000>
- Matsuoka, A., Teramoto, M., Nomura, R., Nose, M., Fujimoto, A., Tanaka, Y., et al. (2018). The ARASE (ERG) magnetic field investigation. *Earth, Planets and Space*, *70*. <https://doi.org/10.1186/s40623-018-0800-1>
- Miyoshi, Y., Hori, T., Shoji, M., Teramoto, M., Chang, T. F., Segawa, T., et al. (2018). The ERG science center. *Earth, Planets and Space*, *70*(1), 96. <https://doi.org/10.1186/s40623-018-0867-8>
- Miyoshi, Y., Sakaguchi, K., Shiokawa, K., Evans, D., Albert, J., Connors, M., & Jordanova, V. (2008). Precipitation of radiation belt electrons by EMIC waves, observed from ground and space. *Geophysical Research Letters*, *35*(23). <https://doi.org/10.1029/2008gl035727>
- Miyoshi, Y., Shinohara, I., & Jun, C.-W. (2018). *The level-2 orbit data of exploration of energization and radiation in geospace (ERG) ARASE satellite* (Version v03, updated daily). ERG Science Center, Institute for Space-Earth Environmental Research, Nagoya University. <https://doi.org/10.34515/DATA.ERG-12000>
- Miyoshi, Y., Shinohara, I., Takashima, T., Asamura, K., Higashio, N., Mitani, T., et al. (2018). Geospace exploration project ERG. *Earth, Planets and Space*, *70*(1), 101. <https://doi.org/10.1186/s40623-018-0862-0>
- Mursula, K., Bräysy, T., Niskala, K., & Russell, C. T. (2001). PC1 pearls revisited: Structured electromagnetic ion cyclotron waves on polar satellite and on ground. *Journal of Geophysical Research*, *106*(A12), 29543–29553. <https://doi.org/10.1029/2000ja003044>
- Nomura, R., Shiokawa, K., Omura, Y., Ebihara, Y., Miyoshi, Y., Sakaguchi, K., et al. (2016). Pulsating proton aurora caused by rising tone PC1 waves. *Journal of Geophysical Research: Space Physics*, *121*(2), 1608–1618. <https://doi.org/10.1002/2015ja021681>
- Obayashi, T. (1965). Hydromagnetic whistlers. *Journal of Geophysical Research*, *70*(5), 1069–1078. <https://doi.org/10.1029/jz070i005p01069>
- Omura, Y., Usui, H., & Matsumoto, H. (1988). Parallel heating associated with interaction of forward and backward electromagnetic cyclotron waves. *Journal of Geomagnetism and Geoelectricity*, *40*(8), 949–961. <https://doi.org/10.5636/jgg.40.949>

- Ozaki, M., Shiokawa, K., Miyoshi, Y., Kataoka, R., Connors, M., Inoue, T., et al. (2018). Discovery of 1 Hz range modulation of isolated proton aurora at subauroral latitudes. *Geophysical Research Letters*, *45*(3), 1209–1217. <https://doi.org/10.1002/2017gl076486>
- Ren, J., Zhou, X.-Z., Zong, Q.-G., Yue, C., Fu, S.-Y., Miyoshi, Y., et al. (2021). The link between wedge-like and nose-like ion spectral structures in the inner magnetosphere. *Geophysical Research Letters*, *48*(13), e2021GL093930. <https://doi.org/10.1029/2021gl093930>
- Sakaguchi, K., Shiokawa, K., Miyoshi, Y., & Connors, M. (2015). Isolated proton auroras and PC1/EMIC waves at subauroral latitudes. In *Auroral dynamics and space weather* (pp. 59–70). American Geophysical Union (AGU). <https://doi.org/10.1002/9781118978719.ch5>
- Shiokawa, K., Katoh, Y., Hamaguchi, Y., Yamamoto, Y., Adachi, T., Ozaki, M., et al. (2017). Ground-based instruments of the PWING project to investigate dynamics of the inner magnetosphere at subauroral latitudes as a part of the ERG-ground coordinated observation network. *Earth, Planets and Space*, *69*(1), 160. <https://doi.org/10.1186/s40623-017-0745-9>
- Spence, H. E., Reeves, G. D., Baker, D. N., Blake, J. B., Bolton, M., Bourdarie, S., et al. (2013). Science goals and overview of the radiation belt storm probes (RBSP) energetic particle, composition, and thermal plasma (ECT) suite on NASA's Van Allen probes mission. *Space Science Reviews*, *179*(1), 311–336. <https://doi.org/10.1007/s11214-013-0007-5>
- Troitskaya, V. A., & Gul'elmi, A. V. (1967). Geomagnetic micropulsations and diagnostics of the magnetosphere. *Space Science Reviews*, *7*(5), 689–768. <https://doi.org/10.1007/BF00542894>
- Tsyganenko, N. (1989). A magnetospheric magnetic field model with a warped tail current sheet. *Planetary and Space Science*, *37*(1), 5–20. [https://doi.org/10.1016/0032-0633\(89\)90066-4](https://doi.org/10.1016/0032-0633(89)90066-4)
- Usanova, M. E., Mann, I. R., Rae, I. J., Kale, Z. C., Angelopoulos, V., Bonnell, J. W., et al. (2008). Multipoint observations of magnetospheric compression-related EMIC PC1 waves by themis and carisma. *Geophysical Research Letters*, *35*(17). <https://doi.org/10.1029/2008gl034458>
- Vines, S. K., Allen, R. C., Anderson, B. J., Engebretson, M. J., Fuselier, S. A., Russell, C. T., et al. (2019). EMIC waves in the outer magnetosphere: Observations of an off-equator source region. *Geophysical Research Letters*, *46*(11), 5707–5716. <https://doi.org/10.1029/2019gl082152>
- Yue, C., Ma, Q., Jun, C.-W., Bortnik, J., Zong, Q., Zhou, X., et al. (2020). The modulation of plasma and waves by background electron density irregularities in the inner magnetosphere. *Geophysical Research Letters*, *47*(15), e2020GL088855. <https://doi.org/10.1029/2020gl088855>
- Zhang, J.-C., Kistler, L. M., Mouikis, C. G., Klecker, B., Sauvaud, J.-A., & Dunlop, M. W. (2011). A statistical study of EMIC wave-associated He+ energization in the outer magnetosphere: Cluster/CODIF observations. *Journal of Geophysical Research*, *116*(A11). <https://doi.org/10.1029/2011ja016690>